Scattering of He^3 from He^4 and States in Be^7†

PHILIP D. MILLER* AND G. C. PHILLIPS
The Rice Institute, Houston, Texas
(Received August 29, 1958)

The range of excitation energies in Be^7 from 3.28 to 4.73 Mev has been investigated by Van de Graaff-accelerated He^{3+} ions scattered from He^4 gas in a differentially pumped, large-volume scattering chamber. The second excited state in Be^7 has been studied, and its laboratory resonant energy and width have been determined to be 5.17 Mev and 0.180 Mev, respectively, corresponding to an excitation energy in Be^7 of 4.53 ± 0.02 Mev and a center-of-mass width of 0.102 Mev. The spin and parity are $J=\frac{7}{2}^-$ and the reduced width is 3.0×10^{-13} Mev-cm. The behavior of the nonresonant phase shifts is shown to be qualitatively consistent with other known states in Be^7, whose resonant energies lie outside the range of the present experiment.

EXPERIMENTAL DATA

IONS of He^{3+} have been scattered from helium gas to investigate low excited states of Be^7. The Rice Institute Van de Graaff accelerator was employed and a large volume scattering chamber was used for the He^3+He^4 scattering experiments; this chamber and the techniques have been described in detail by Russell *et al.*[1] The similarity of the masses of He^3 and He^4 produced the principal experimental difficulties of the present experiment. At forward angles the energy of recoil He^4 nuclei and the energy of scattered He^3 nuclei are so similar that the two groups of particles entering the CsI(Tl) scintillation detector could not be satisfactorily resolved using pulse height analysis alone, while at backward angles the scattered He^3 nuclei have such low energies (1/49 of the incident energy at 180°) that their pulses were indistinguishable from noise. For these reasons it was decided to count the scattered He^3 nuclei and the recoil He^4 nuclei in coincidence. A variable slit system with six different slit widths was constructed for use with one of the detectors in the scattering chamber (detector No. 2) and allowed data to be obtained between 50° and 130° in the center-of-mass system.

Coincidence losses, and the high background at backward angles, makes an estimate of the errors in the present experiment difficult. However, a reasonable estimate of the probable error is $\pm5\%$ from 70° to 90° in the center-of-mass system and $\pm10\%$ outside of this range.

Two angular distributions at 2.97- and 3.88-Mev bombarding energy and six excitation curves at center-of-mass angles 54°44′, 63°26′, 90°, 109°52′, 116°34′, and 125°16′ constitute the data for the $He^4(He^3,He^3)He^4$ experiment. All but the last of the above excitation curves cover the bombarding energy range from 3.0 to 5.5 Mev, while the excitation curve at 125°16′ spans the bombarding energy range from 4.5 to 5.5 Mev. The two excitation curves at the most forward angles were obtained by counting the recoil He^4 nuclei in detector No. 1 with the coincident He^3 nuclei in detector No. 2, while the rest of the excitation curves were obtained by counting the scattered He^3 nuclei in detector No. 1 with the coincident He^4 nuclei in detector No. 2. Figure 1 shows the two angular distributions with both the points obtained by counting He^3 nuclei in detector No. 1, and the points obtained by counting He^4 nuclei in detector No. 1. Figure 2 shows the excitation curves. Smooth curves have been drawn through the data points and their use in the phase shift analysis will be described in the next section.

The energy scale, as determined by magnetic analysis of He^3-induced charged-particle reactions,[2,3] was known to ±20 kev.

THE PHASE-SHIFT ANALYSIS

The formula for the differential cross section in the center-of-mass system, as a function of the nuclear phase shifts, has been given in a number of other papers.[4,5]

The program for an IBM 650 computer for extracting phase shifts using the partial waves through $l=4$ is described in the previous communication. The phase-shift fits to the 2.97- and 3.88-Mev angular distributions are shown in Fig. 1.

Smooth curves were drawn through the data points of the excitation curves, and angular distributions were formed at convenient energy intervals. A least-squares phase-shift analysis was made of these angular distributions. It was found that the nonresonant phase shifts fluctuated in going across the resonance due to small energy-scale errors of the excitation curves. For this reason, smooth curves were drawn through the nonresonant phase shifts such that more weight was given to those points below and above the resonance. Thus the errors in the phase shifts, due to small errors

† Supported in part by the U. S. Atomic Energy Commission.
* Now with the Oak Ridge National Laboratory, Oak Ridge, Tennessee.
[1] Russell, Phillips, and Reich, Phys. Rev. 104, 135 (1956).

[2] R. R. Spencer, Ph.D. thesis, The Rice Institute, 1958 (unpublished).
[3] T. E. Young, Ph.D. thesis, The Rice Institute, 1958 (unpublished).
[4] C. L. Critchfield and D. C. Dodder, Phys. Rev. 76, 602 (1949).
[5] P. D. Miller and G. C. Phillips, preceding paper [Phys. Rev. 112, 2043 (1958)].

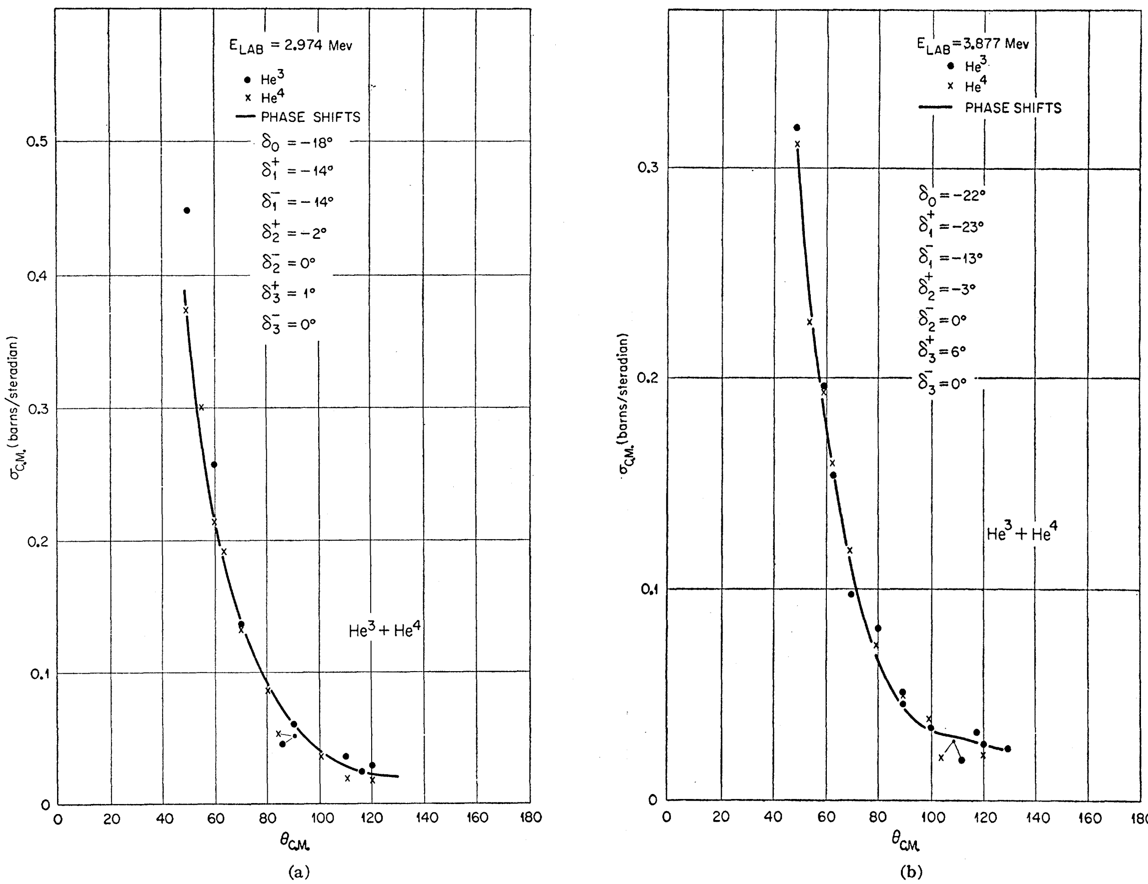

FIG. 1. $He^4(He^3,He^3)He^4$ angular distributions at 2.97- and 3.88-Mev bombarding energy. The center-of-mass cross sections are plotted *versus* the center-of-mass angles. Points observed by counting scattered He^3 nuclei and by counting recoil He^4 nuclei, as discussed in the text, are both shown. Phase-shift fits to the angular distributions, for the phase shifts given, are shown.

in relative energy scales of the different excitation curves, were a minimum. The resulting nonresonant phase shifts were then used as trial values and only δ_3^+ was allowed to vary. Then these values of δ_3^+ were employed and each of the other shifts was fitted in turn to the data. These final phase shifts are shown in Fig. 3.

INTERPRETATION OF THE PHASE SHIFTS

S Wave

The accuracy of the *S*-wave phase shifts are estimated from the dispersion of the points in Fig. 3(a) to be about $\pm 4°$. Within this accuracy the phase shifts due to a charged hard sphere with a radius of 2.8×10^{-13} cm fits the experimental points satisfactorily. The small radius for the *S* wave phase shift is rather puzzling, but the same result for the *S*-wave seems to apply to other problems involving alpha particles and light projectiles; for example, for $p+He^4$ scattering a radius of 2.0×10^{-13} cm was deduced,[5] while for He^4+He^4 scattering a radius of 4.4×10^{-13} cm has been reported.[6]

[6] Nilson, Jentschke, Briggs, Kerman, and Snyder, Phys. Rev. **109**, 850 (1958).

P Wave

The *P*-wave phase shifts are shown in Fig. 3(b). The splitting between δ_1^+ and δ_1^-, corresponding to $J=\frac{3}{2}-$ and $J=\frac{1}{2}-$, respectively, seems to be significant over the entire energy range covered by the present experiment. The fact that the splitting between the two *P*-wave phase shifts is relatively constant over this energy range and the fact that both slopes of the phase shifts with respect to the energy are relatively constant, suggest that the splitting is due to the ground and first excited states of Be^7 rather than to higher states. Furthermore, there are apparently[7,8] no other $\frac{1}{2}-$ or $\frac{3}{2}-$ states below 8.6 Mev of excitation in Be^7. It will be assumed for the purposes of the present analysis that the splitting of the *P*-wave phase shifts is due entirely to the ground and first excited states of Be^7. The dispersion theory formulas for the phase shifts have been given in the previous paper[5] as Eqs. (5) through (9).

In order to evaluate the characteristic energies, E_λ, in these formulas, it was necessary to evaluate the level shift Δ_λ at the negative resonant energy. The level

[7] S. Bashkin and H. T. Richards, Phys. Rev. **84**, 1124 (1951).
[8] Marion, Weber, and Mozer, Phys. Rev. **104**, 1402 (1956).

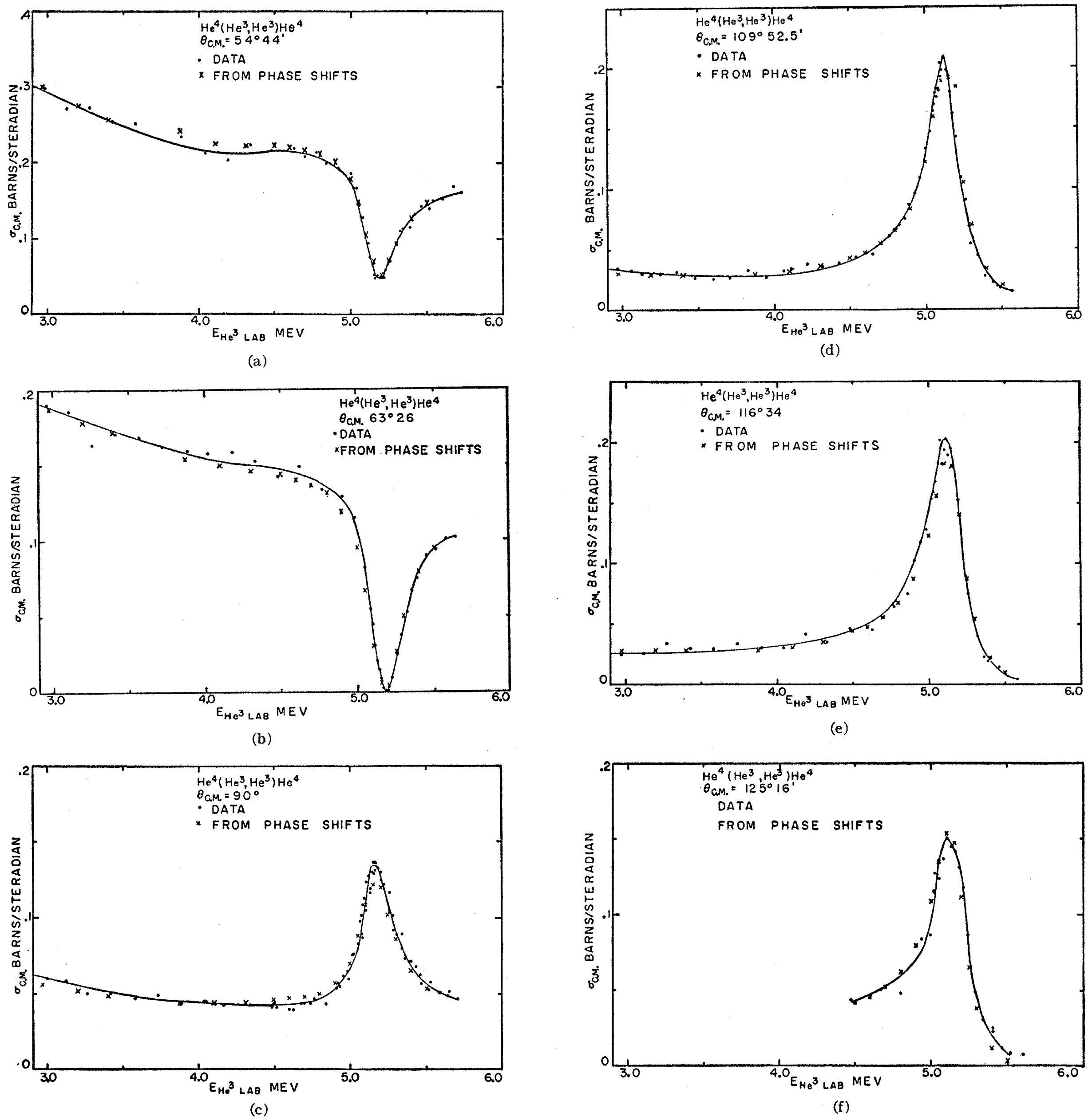

FIG. 2. $He^4(He^3,He^3)He^4$ excitation curves at six center-of-mass angles. The center-of-mass cross sections are plotted *versus* bombarding energy. The use of the smooth curves in the phase-shift analysis is described in the text. Phase-shift fits to the excitation curves are given for the phase shifts shown in Fig. 3, and are shown as crosses.

shift in this case is given by[9]

$$\Delta_\lambda = -(\gamma_\lambda^2/R)[(\rho W'/W)+l], \quad (1)$$

where W is the Whittaker function, $W_{-\eta,\, l+\frac{1}{2}}(2\rho)$. The quantities entering (1) are

$$\rho = kR,$$
$$k = (2\mu|E_{\mathrm{c.m.}}|/\hbar^2)^{\frac{1}{2}},$$
$$\eta = \mu Z_1 Z_2 e^2/\hbar k.$$

[9] R. G. Thomas, Phys. Rev. 88, 1109 (1952).

The WKB approximation to the negative energy shift function has also been evaluated by Thomas,[9] and the result is

$$\rho W'/W = -\xi + \tfrac{1}{2}[\rho\eta + (l+\tfrac{1}{2})^2]\xi^{-2}, \quad (2)$$

where

$$\xi = [(l+\tfrac{1}{2})^2 + 2\rho\eta + \rho^2]^{\frac{1}{2}}.$$

The values of E_λ for the ground and 430-kev first excited states of Be^7 were computed using 1.583 Mev as

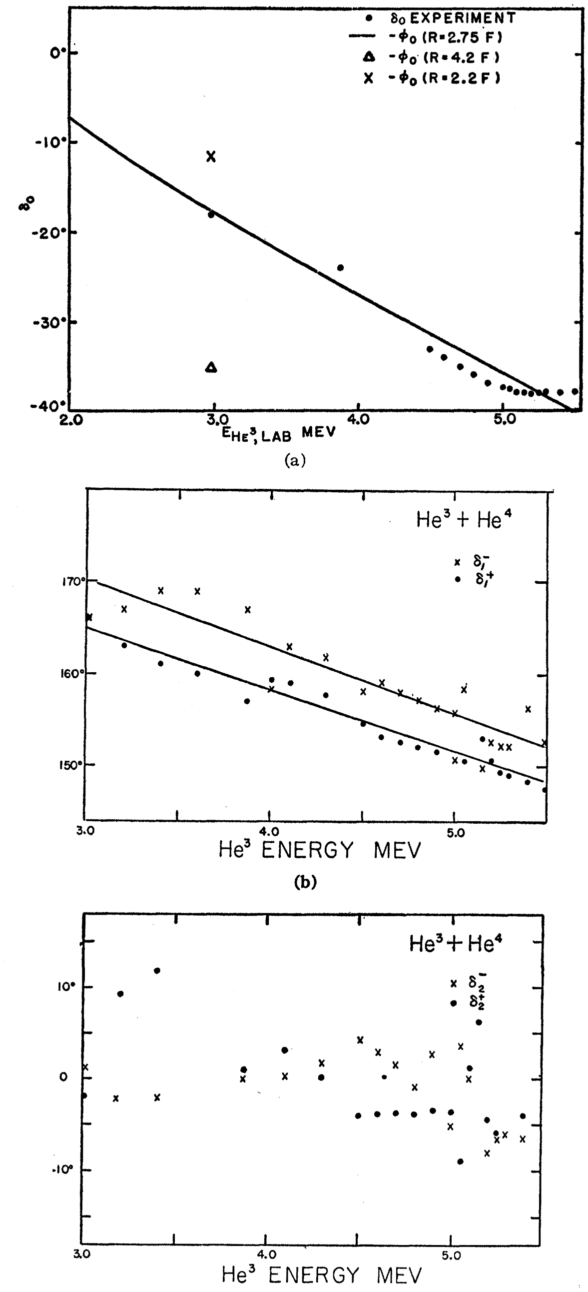

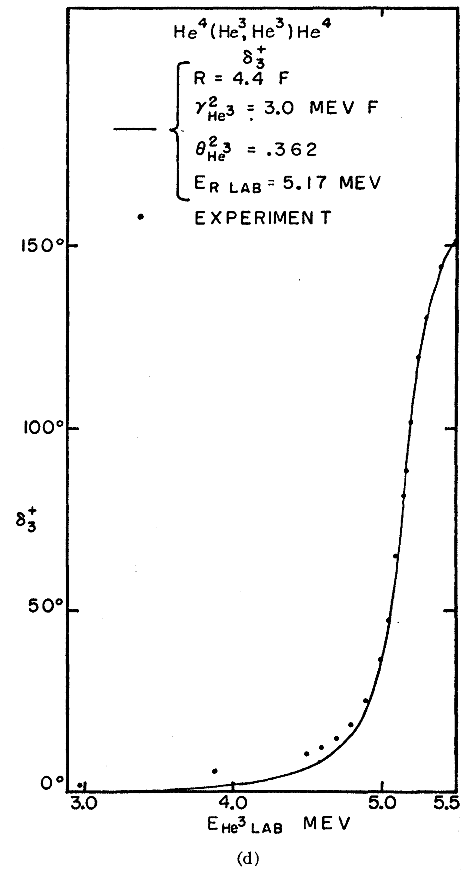

FIG. 3. $He^4(He^3,He^3)He^4$ phase shifts plotted *versus* bombarding energy. Hard-sphere fits are presented for the *S*-wave phase shift, while the *P*-wave phase shifts are fitted to straight lines by least squares. Dispersion-theory fits are given for the *F* waves. The parameters and techniques used for obtaining fits to the data points are discussed in the text. The radius *R* is given in fermis [1 fermi (f) $\equiv 10^{-13}$ cm].

the value of the He^3+He^4 threshold, and using (1) and (2) above.

Figure 4 shows δ_1^+ and δ_1^- plotted on separate scales. The dotted lines in the figure are arbitrarily adopted, for the purposes of this analysis, as the greatest limits of fluctuation about the least-squares fits that a dispersion theory fit may have in order to be acceptable.

Reference to some of the dispersion theory points in Fig. 4 shows that they also lie on very straight lines. Various values of the nuclear radius, *R*, and of the reduced widths, $(\gamma_{\lambda=He^3})^2$, were tried, and were considered acceptable if the slopes and values of the *P*-wave phase shifts between 3.0 and 5.5 Mev were reasonably close to the dashed limits shown in Fig. 4. Only values of the reduced widths less than the Winger limit[10] were explored. The results of these calculations are shown in Fig. 5, where the acceptable regions are shown plotted on coordinates of γ_λ^2 *versus* *R*. The lines of best fit are the heavy lines within each region. Thus, it seems very possible that the ground state, and possibly the first

[10] T. Teichmann and E. P. Wigner, Phys. Rev. **87**, 123 (1952).

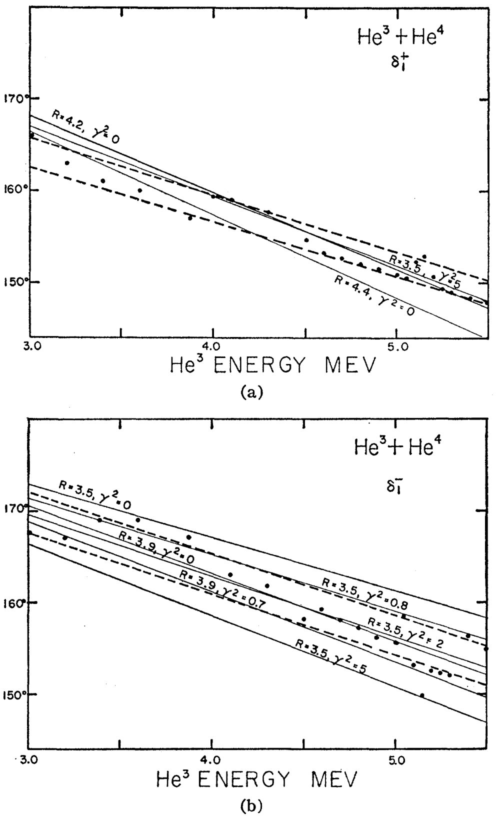

FIG. 4. The P-wave experimental phase shifts are shown with some fits attempted using dispersion theory and with acceptance limits as discussed in the text. (R in fermis; γ^2 in Mev f.)

excited state, have widths which are an appreciable fraction of the He^3+He^4 single-particle limit.

D Waves

The D-wave phase shifts are shown in Fig. 3(c). The scatter of the experimental points is such that nothing may be said concerning their interpretation.

F Waves

The $F_{7/2}$ phase shift is shown in Fig. 3(d). Since the least squares fit to the $F_{\frac{5}{2}}$ phase shift resulted in values that fluctuated within 2° around 0°, δ_3^- was constrained to be zero. A reasonable dispersion theory fit to δ_3^+ is shown in Fig. 3(d). The resonant bombarding energy is 5.17 Mev, corresponding to an excitation energy in Be^7 of 4.53 ± 0.02 Mev. Using an F-wave radius of $R=4.4\times10^{-13}$ cm, the level parameters which have been extracted are $(\gamma_{He^3})^2=3.0\times10^{-13}$ Mev-cm, $E_\lambda=3.43$ Mev, and $(\theta_{He^3})^2=0.36$, where the last parameter is the ratio of the reduced width of the state to the Wigner limit. It is, perhaps, remarkable that this state, which agrees in spin, parity, and energy with the shell-model predictions of Inglis,[11] should be such a good single-particle state of He^3+He^4.

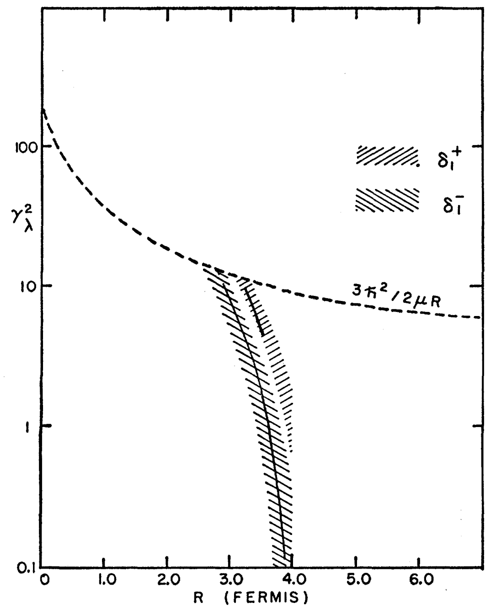

FIG. 5. Acceptable He^3+He^4 parameters for the ground and first excited states of Be^7 as determined by the elastic scattering of He^3 from He^4. The solid lines shown within each region of acceptable P-wave parameters are the best least-squares fits to the straight lines of Fig. 3(b).

[11] D. R. Inglis, Revs. Modern Phys. 25, 390 (1953).